Comparisons of Scatterometer and TAO Winds Reveal Time-Varying Surface Currents for the Tropical Pacific Ocean

Kathryn A. Kelly

Applied Physics Laboratory, University of Washington, Seattle, Washington, USA

Suzanne Dickinson

Applied Physics Laboratory, University of Washington, Seattle, Washington, USA

Gregory C. Johnson

Pacific Marine Environmental Laboratory, NOAA, Seattle, Washington, USA

Revised for Journal of Atmospheric and Oceanic Technology

July 2, 2004

Abstract.
The differences between Tropical Atmosphere-Ocean (TAO) anemometer and QuikSCAT scatterometer winds are analyzed over a period of three years. Systematic differences are expected owing to ocean currents because the anemometer measures absolute air motion, whereas a radar measures the motion of the air relative to the ocean. Monthly averaged collocated wind differences (CWDs) are compared with available near-surface current data: at 15-m depth from drifters, at 25-m depth from acoustic Doppler current profilers (ADCPs), at 10-m depth from current meters, and geostrophic currents at the surface from the TOPEX/Poseidon radar altimeter. Because direct current observations are so sparse, we also make comparisons with climatological currents from these same sources. Zonal CWDs are in good agreement with the zonal current observations, particularly from 2°S to 2°Nwhere there are strong currents and a robust seasonal cycle, with the altimeter-derived anomalous currents giving the best match. At higher latitudes there is qualitative agreement at buoys with relatively large currents. The overall variance of the zonal component of the CWDs is reduced by approximately 25% by subtracting an estimate of the zonal currents. The meridional CWDs are nearly as large as the zonal CWDs, but are unpredictable. The mean CWDs show a robust divergence pattern about the equator, which is suggestive of Ekman currents, but with unexpectedly large magnitudes.
Coefficients for estimating climatological zonal surface currents from the altimeter at the TAO buoys are tabulated: the amplitudes and phases for the annual and semi-annual harmonics, and a linear regression against the Southern Oscillation Index are combined with the mean from the drifter currents. Examples are shown of the application of these estimators to data from SeaWinds on the Midori satellite. These estimators are also useful for deriving air-sea fluxes from TAO winds.

1. Introduction

The radar scatterometer measures backscatter from centimeter-scale waves caused by the wind blowing over the ocean; when ocean and atmosphere move together, no waves are generated and no wind is measured. An anemometer, on the other hand, measures the motion of the air relative to a fixed platform. When the wind blows against (with) the surface currents, the scatterometer will measure higher (lower) wind than an anemometer on a buoy. If ocean currents are the dominant source of discrepancies between the two wind measurements, then the difference (anemometer minus scatterometer) should agree with estimates of the ocean surface currents. Differences between the wind vectors from the Tropical Atmosphere-Ocean (TAO) buoys and from the SeaWinds scatterometer are compared here with time-varying ocean surface currents over a three-year period beginning with the start of the QuikSCAT mission in July 1999.

For purposes of computing air-sea fluxes, the measurement of the relative motion by the scatterometer has an advantage over an anemometer wind. In bulk parameterizations, (e.g., Liu et al., 1979) surface stress τ and all other air-sea fluxes are a function of the difference between the wind at a reference height $\mathbf{U}$ and the current at the ocean surface $\mathbf{U_s}$, as

$$\tau = \rho C_D |\mathbf{U} - \mathbf{U_s}| (\mathbf{U} - \mathbf{U_s}) \quad (1)$$

The wind derived from the scatterometer backscatter represents the relative motion, $\mathbf{U} - \mathbf{U_s}$. To derive stress from an anemometer wind or from any other absolute wind measurement, it is necessary to subtract an estimate of the ocean surface current. The relative motion, $\mathbf{U} - \mathbf{U_s}$, is also needed for other bulk flux formulas. The ocean currents are frequently neglected in the bulk formula, because ocean surface currents are not readily available; however, a combination of weak winds and strong currents will give large errors in these flux estimates.

Previous comparisons between TAO and scatterometer winds with currents using relatively small amounts of data suggested an important role for currents in the difference. Collocated wind differences (CWDs hereafter) from the NASA Scatterometer (NSCAT) and TAO anemometers showed qualitative agreement with currents from a single current meter on the equator over a 7-month period, as currents reversed during the onset of the 1997 ENSO warm event (Dickinson et al., 2001). Similarly, good agreement was found between QuikSCAT winds and currents from an acoustic Doppler current profiler (ADCP) mounted on a ship servicing the TAO array, averaged over a 3-week period (Kelly et al., 2001). In the comparison with QuikSCAT winds, currents in the South Equatorial Current (SEC) were about 1.2 ms^{-1} westward and currents in the North Equatorial Countercurrent (NECC) were about 0.6 ms^{-1} eastward over the short period examined. Neglect of these strong equatorial currents in this region of relatively weak winds (5-7 ms^{-1}) were estimated to cause errors in stress of 25-50% and even larger errors in wind stress curl.

Here, we compare three years of CWDs with surface currents at most of the TAO buoys. The CWDs, which are computed from the difference of two observations, are likely to be noisier than either; in fact, if the error variance for the anemometer is ϵ_a^2 and the error variance for the scatterometer is ϵ_s^2, then the error variance for the current estimate is $\epsilon_a^2 + \epsilon_s^2$, assuming these errors are uncorrelated. Therefore, it was necessary to edit and temporally average the CWDs for the comparisons.

The goals of this analysis are 1) to demonstrate that systematic differences between (zonal) TAO anemometer and QuikSCAT winds are from time-varying ocean currents, 2) to find (and provide) appropriate current estimators to convert between the relative scatterometer and absolute anemometer winds, and 3) to demonstrate the need to include ocean currents in anemometer/scatterometer validation studies.

Although TAO buoys are not used in the calibration of the scatterometer model function (see, for example, Wentz and Smith, 1999), which relates direction and speed to radar backscatter, they are used to "validate" the winds. The model function is based on global collocated backscatter with several months of wind vectors from numerical weather prediction models; the calibration is a highly overdetermined problem with most of the winds from regions of weak ocean currents. To illustrate the independence of the buoy and scatterometer winds, we note that the ERS-1, NSCAT, and QuikSCAT scatterometers all showed systematic direction biases to the right of the TAO anemometers of approximately 9-11°, a remarkable consistency. Subsequent analyses of the accuracy of the ATLAS anemometers revealed a 6.8° bias to the left (Freitag et al., 2001), accounting for much of what was observed by the scatterometers. (This direction error has been corrected in the TAO winds.)

Anemometer winds are used to check the scatterometer speed and direction accuracy ("validation") and, therefore, it is critical that we understand the nature of the differences in the measurements. In the validation of the NSCAT model function, initial TAO buoy/NSCAT comparisons suggested that the scatterometer winds were too low by about 0.5 ms^{-1}. However, after equa-

torial currents reversed early in 1997, scatterometer winds appeared to be too high as would be expected for a relative motion measurement, demonstrating the need to include ocean currents in the comparisons. In the QuikSCAT validation, after removing the measured currents in the CWDs, we found the model function bias was a negligible 0.1 ms^{-1} (Kelly et al., 2001).

The need for a conversion between buoy and scatterometer winds also arises in the evaluation of flux products. In bulk formulas for estimating latent and sensible heat fluxes, for example, the relative motion $\mathbf{U} - \mathbf{U_s}$ is also needed. At 140°W on the equator, where current measurements are available, latent heat flux estimated with and without these energetic ocean currents had a seasonally varying difference with amplitude of about 7 Wm^{-2} and a mean of 2 Wm^{-2} (M. Cronin, personal communication, 2004). To determine, for example, whether the use of scatterometer winds improves air-sea flux products, as in recent studies by Yu et al. (2004), an accurate comparison with fluxes from a bulk formula at a TAO buoy would also require a current estimate (few TAO buoys have current meters).

2. Collocated wind vectors

The TAO buoys used in this study are located in the equatorial Pacific Ocean bounded by 165°E, 95°W, 8°S, and 12°N. High resolution TAO buoy data were collected from the beginning of the QuikSCAT mission, July 1999, through August, 2002. The buoy data include zonal and meridional wind components, air temperature, sea surface temperature and relative humidity. The sampling rate for all variables except the sea surface temperature is 2 Hz, with a sampling period of two minutes. Data are recorded every ten minutes. The sea surface temperature data are instantaneous measurements taken once every ten minutes. The winds, which are measured at a height of four meters above the ocean surface, are converted to a 10-m height in a neutrally stratified atmosphere using the standard LKB algorithm (Liu et al., 1979). The 6.8° wind direction bias (Freitag et al., 2001) has been removed from the TAO data. TAO winds are temporally averaged to give hourly winds.

QuikSCAT scatterometer wind speed and direction data (standard L2B product from PODAAC; Wentz and Smith, 1999; Huddleston et al., 1999) were collected over the three-year time period. The scatterometer data are calibrated to approximate a wind at 10 m above the ocean surface in a neutrally stratified atmosphere and have a spatial resolution of 25 km. Data pairs were considered collocated when the scatterometer cell center was within 25 km of a buoy and the time difference was less than 30 minutes, giving a unique pairing with the hourly TAO winds.

The collocated pairs were screened for rain, wind direction, and wind speed. The rain screen was performed using collocated rain estimates derived from the Special Sensor Microwave Imager (SSM/I) (courtesy of Remote Sensing Systems). The rain estimates consist of a rain rate (or designation of "no rain") and the time difference between the SSM/I and the scatterometer measurement (maximum of three hours). Because we only used CWDs for which there was a rain estimate indicating "no rain detected within 50 km" of the scatterometer vector, there was a tradeoff between reducing rain contamination (and therefore the variance of the CWDs) by selecting a short time difference and the amount of data available for our analysis. We examined the variance of the CWDs for maximum time differences of 30, 60, 120, or 180 minutes; the CWD variance for the less-stringent 180-minute time window was only a few percent higher than the variance for the 30-minute time window, but the number of CWDs was double that for the 30-minute window. The negligible increase in variance suggests that using the less restrictive 3-hr time window does not degrade the scatterometer wind quality. Therefore, to maximize the amount of data for analysis, a collocated buoy/scatterometer pair was included if there was a SSM/I estimate within three hours of the scatterometer measurement that indicated no rain was present.

The scatterometer model function gives up to four possible wind vectors, owing to the similarity of the backscatter from different viewing geometries. To ensure that the correct scatterometer vector was selected, the collocated pair was retained only if the difference in the wind directions between buoy and scatterometer was less than 60°. Lastly, if the buoy wind speed was 3 ms^{-1} or less the pair was excluded owing to the difficulty of both sensors in measuring directions for low wind speeds. Of the initial collocations, 10% had buoy wind speeds below the threshold, 6% had directional differences that were too large, and 18% had no SSM/I flag within 3 hours or the SSM/I flag indicated rain. Overall, 74% of the pairs met the above requirements, resulting in a data set of 28,031 collocated wind pairs.

Tropical Pacific Ocean CWDs were estimated by subtracting QuikSCAT scatterometer wind vectors from collocated TAO vectors at 56 TAO buoys. Even after the screening described above, the screened CWDs were quite noisy. To reduce the noise CWDs with speeds of 2 ms^{-1} or greater were removed, as these represent unrealistically large values for ocean currents and were suspected to be contaminated by a noise source such as un-

detected rain. In addition, a two-month running mean at monthly intervals was computed for the zonal and meridional components and three-standard-deviation outliers from these means were removed. These criteria eliminated 15% of the remaining data. The two-month running mean was computed on the remaining CWDs and these monthly means were used for comparisons with ocean currents.

3. Current Observations

There are several sources of near-surface velocity measurements available for comparisons: moored and shipboard acoustic Doppler current profiler (ADCP), drifters, one current meter, and altimetric sea surface height. Moored ADCP data were available at four equatorial buoys in our domain. A single current meter at 110°W on the equator measured 10-m currents for a few months in 2001, allowing another comparison.

Because so few direct current measurements were available at the TAO buoys during our study period, we used current estimates from the other data sources. Currents at 15 meters from the drogued drifters of the Global Drifter Program were daily-averaged and fit to a function in time and space (Johnson, 2001). The mean, annual and semi-annual harmonics, and an SOI regression coefficient for both zonal and meridional currents were estimated at the TAO buoy locations from over two decades of data. From the zonal coefficients we constructed a climatological drifter current time series.

We also examined current estimates from shipboard ADCP data from the shallowest depth at 25 meters. Climatological zonal velocities were constructed from 172 longitudinal transects of shipboard ADCP data from 1985 though 2001 based on a regression analysis (Johnson et al, 2002). Meridional ADCP currents are badly aliased by sparse sampling in the presence of strong tropical instability waves (TIWs) and the resulting climatological meridional estimates are weak.

Sea surface height (SSH) data measured by the TOPEX/Poseidon altimeter were used to compute anomalous geostrophic ocean surface currents, with the following set of equations,

$$u_g = \frac{-g}{f}\frac{\partial \eta}{\partial y}$$
$$v_g = \frac{g}{f}\frac{\partial \eta}{\partial x} \qquad (2)$$

where η is the SSH anomaly and f is the Coriolis parameter. At the equator, where f is zero, the usual revised formulation was used for the zonal currents, as

$$\beta u_g = -g\frac{\partial^2 \eta}{\partial y^2} \qquad (3)$$

where $\beta = \partial f/\partial y$. An equivalent relationship exists for the meridional component, which includes higher derivatives of the SSH data and is therefore noisy. However, it was not used because, as discussed below, meridional currents do not appear to be geostrophic.

We compared SSH data from the beginning of the QuikSCAT mission (July 1999 through the middle of 2002), with a resolution of 6°×6°×30 days, mapped to a 1°×1°×10 day grid, centered on the half degree (courtesy of M. Schlax and D. Chelton). The four data records surrounding each buoy location were averaged. The monthly velocity estimates were smoothed using a two-month running mean. We also used the entire record of the altimeter data (ten years) to compute the climatological current estimates as described below.

4. Comparisons of the Means

The three-year mean CWDs (Figure 1a) have a similar pattern to that found by Quilfen et al. (2001). To determine to what extent this CWD pattern was affected by using a relatively small subset of the wind data (collocated pairs), we compared the difference of the TAO daily winds and the QuikSCAT daily winds derived from gridded maps (Figure 1b) (Kelly et al., 1999). In the both cases, the annual and semi-annual harmonics were first removed before computing the mean to prevent the seasonal cycle for partial years from biasing the estimate. The mean wind difference maps are quite similar overall, suggesting that the set of CWDs is sufficiently large to give a robust estimate of the difference field.

The CWDs are compared with the means from the climatological drifter estimates in Figure 1c. The zonal CWD and drifter mean currents are similar: predominantly westward along the equator (South Equatorial Current), and predominantly eastward at 5°N and 8°N (North Equatorial Countercurrent), with magnitudes of about 0.5 ms^{-1}. However, there are much larger meridional components in the CWDs than in the drifter means. Both are in the sense of an Ekman divergence driven by easterly trade winds. The mean CWDs are far more divergent about the equator than the mean drifter currents. Given the differences in the mean components, we discuss the comparisons of each component separately below.

5. Zonal Comparisons

We present the time series of zonal CWDs and the zonal velocity observations described above at each buoy location, with plots laid out geographically (upper panels of Figure 2). Plots from a buoy are shown

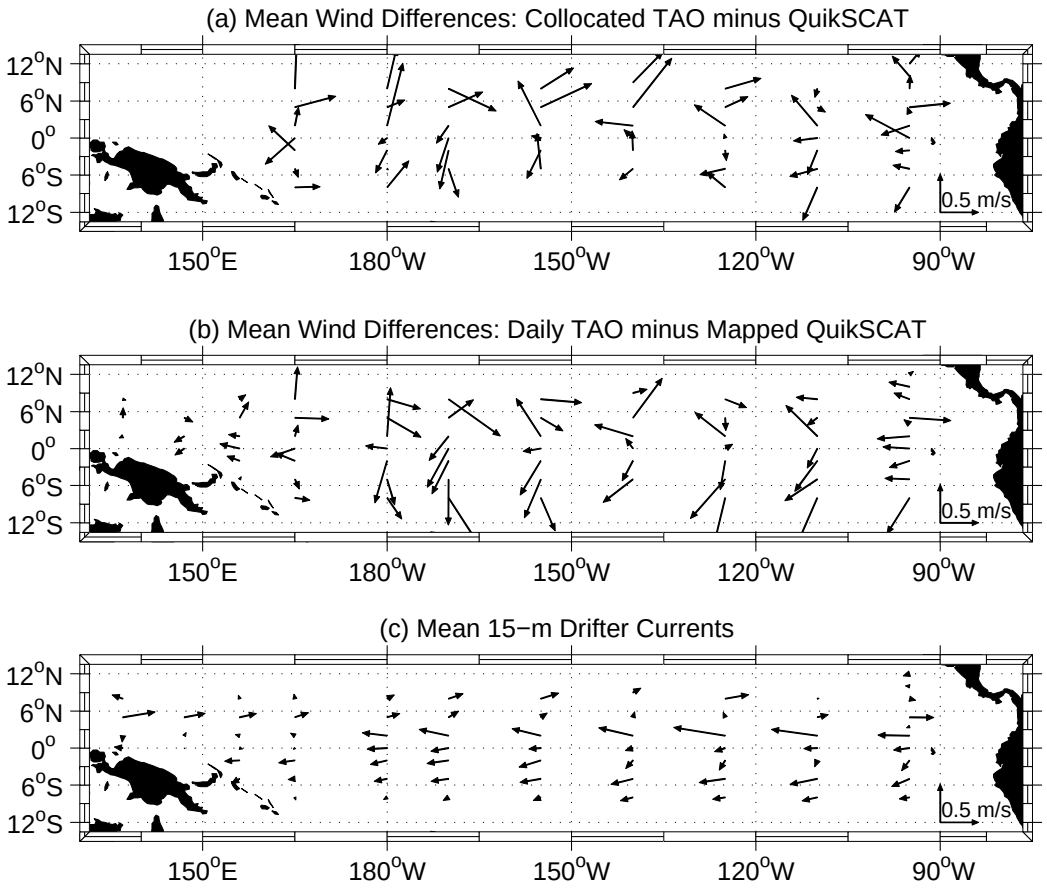

Figure 1. Estimated mean currents. Difference between TAO and QuikSCAT winds for (a) collocated pairs of vectors from July 1999 – August 2002 and (b) all daily TAO winds and QuikSCAT winds from gridded fields for July 1999 – August 2003. (c) Mean currents from 15-m deep drifters at the TAO mooring locations.

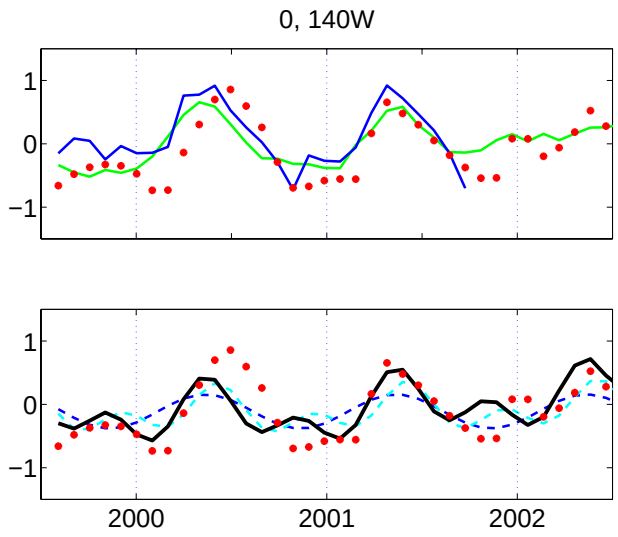

Figure 3. As in Figure 2, for just the TAO buoy at 140°W on the equator.

if the CWDs are available for at least two-thirds of the three-year record. Missing buoy winds generally limit the number of collocations. At most buoys only the geostrophic current anomalies are available; geostrophic velocity estimates have zero mean because they are derived from SSH anomalies relative to a 10-yr record mean. The CWDs show good agreement, particularly in the seasonal cycle, with the observed zonal velocities. At 170, 140 and 110°W on the equator, where some moored ADCP data are also available, all of the velocity estimates are quite similar in phase and in magnitude. There is also good agreement with the 10-m currents at 110°W on the equator. The comparison at 140°W is enlarged (Figure 3) to highlight the long ADCP record.

To allow comparisons with the sparse drifter and shipboard ADCP data, climatological current estimates were computed (lower panels of Figures 2 and 3). The drifter estimator (Johnson, 2001) consists of a mean, an annual and a semi-annual harmonic, and a factor correlated with the Southern Oscillation Index. The ADCP estimator has only a mean and an annual harmonic. The advantage of using estimators is that a current estimate can readily be derived for any TAO buoy at any time, if there are no concurrent velocity observations.

A similar estimator is derived from the geostrophic currents by regressions, using

$$U_s(t) = a_1 \cos(2\pi t/T + \phi_1) + a_2 \cos(4\pi t/T + \phi_2) + b\,SOI + c \quad (4)$$

where the coefficients a_1, ϕ_1, a_2, and ϕ_2 are the amplitude and phase for the annual and semi-annual harmonics, b is derived from a linear regression against the SOI index, and c is the mean. The time t is in days ($t = 0$ corresponds to the start of any given year), $T = 365.25$, and the SOI index is interpolated to the times t. We use SSH data for nearly 10 years (November 1992 through the middle of 2002) to derive the coefficients. Because the geostrophic currents lack a mean, the drifter mean is used in the altimeter estimator.

The CWDs and the velocity data tend to be larger than the climatological estimators, which are derived from regressions. Of the three estimators, the one derived from the altimeter (a surface velocity estimate with a long and complete record) generally has the largest amplitudes, followed by the drifter, with the ADCP estimates having the smallest amplitudes. The reduction in amplitudes for the ADCP and drifter estimators is owing in part to the need to fit the sparse data to a spatial function. However, geostrophic velocities may exceed the actual velocities (Lagerloef et al., 1999; Bonjean and Lagerloef, 2002), because the dynamical balances even as far as 2° from the equator are not simple.

Statistics of the comparisons between CWDs and currents are included in Table 1, which gives the fraction of the variance ("skill") in zonal CWDs described by three different current estimators. Skill is defined here as

$$skill = 1 - \frac{<\epsilon^2>}{\sigma^2} \quad (5)$$

where the error ϵ is the estimated current minus the CWD, σ^2 is the variance of the CWD, and $< \cdot >$ is the ensemble average. In this context, the skill represents the reduction in CWD variance that results from subtracting a given ocean current estimator. The skill, or variance reduction, is given instead of a correlation because it is a more stringent test, penalizing errors in both the mean of the estimator and its amplitude; an estimator that is much too small, for example, can have a high correlation, but it will have a low skill (a small reduction in CWD variance).

Skill is 23% for the drifters overall and 16% for the altimeter (with the drifter mean). The ADCP estimator has no significant skill. Although the skill of the drifter estimator is larger than that for the altimeter, the amplitudes of the altimeter estimates are much closer to the amplitudes of the CWDs. The skill is quite sensitive to the mean difference between the CWDs and the estimator. The drifter means are more westward than the means of the CWDs by an average of 0.09 ms^{-1}. Adding 0.1 ms^{-1} everywhere to the altimeter estimates increases the skill to 28% (Table 1). Despite the strong qualitative resemblance between CWDs and altimeter estimators from 2°S to 2°N, skill is not higher there than for the overall average because a few buoys (2°N,

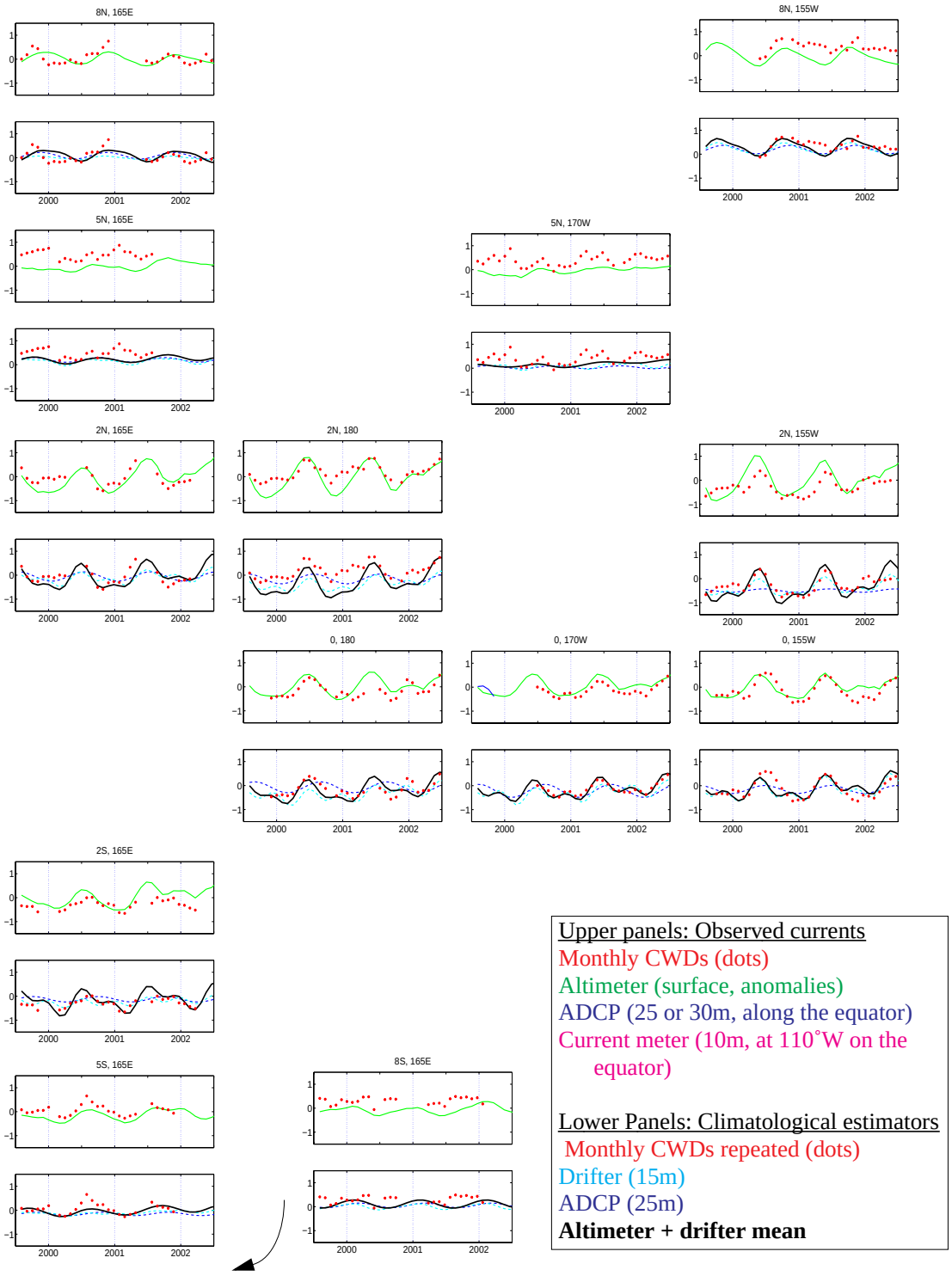

Figure 2. Zonal wind differences and velocities at TAO buoys. Panels are laid out geographically to represent TAO buoy locations. (Upper panels) Monthly CWDs (red dots), geostrophic current anomalies (green), ADCP (blue), and current meter (magenta) on the equator at 110°W and 140°W. Geostrophic currents have zero mean. (Lower panels) Monthly CWDs (repeated), current estimators from ADCP (blue dashed), drifters (cyan dashed), and geostrophic with drifter mean (black). Units are ms^{-1}.

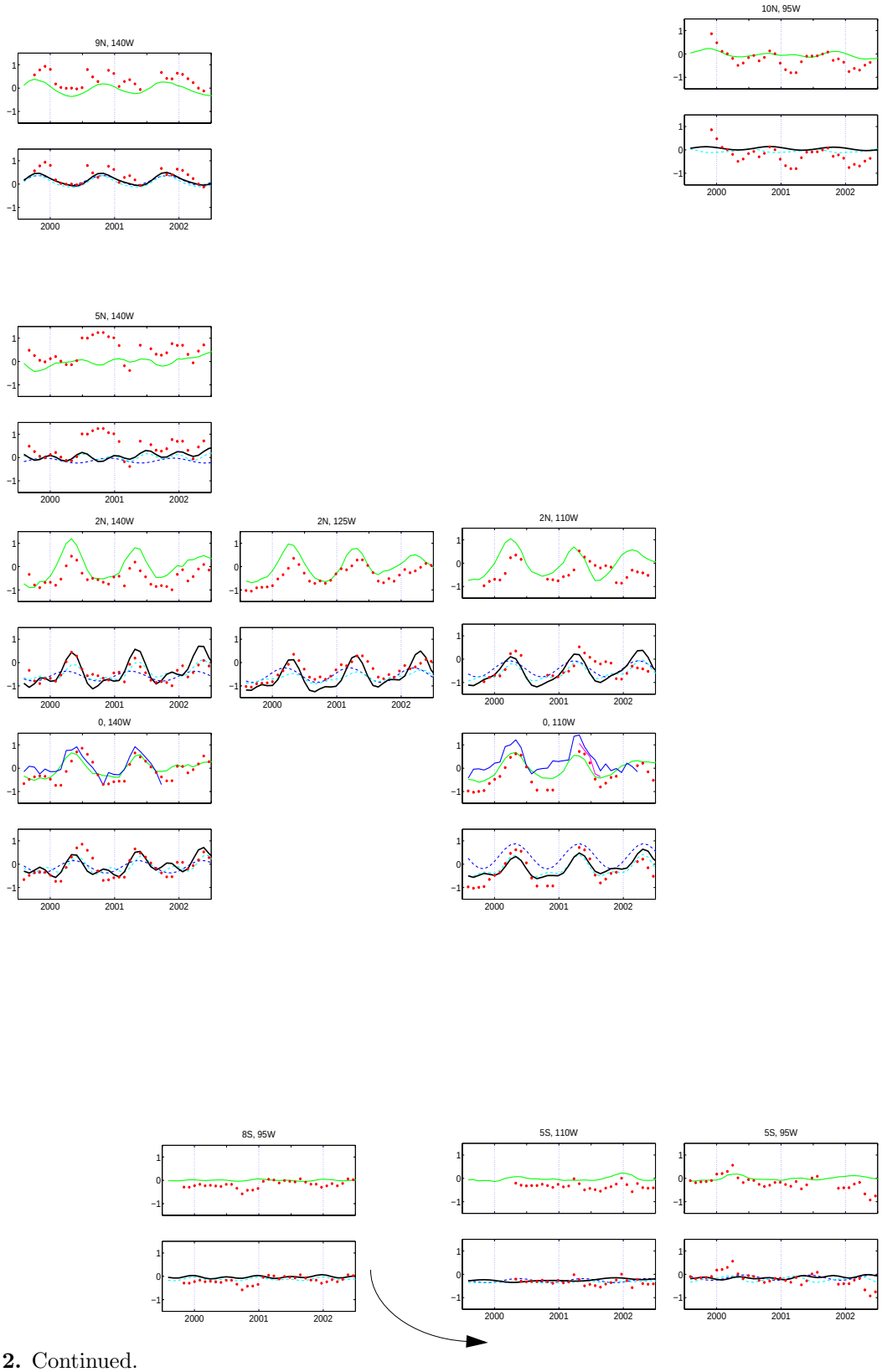

Figure 2. Continued.

Table 1. Skill of estimators

Data for estimator	Skill
drifters	0.23
altimeter + drifter mean	0.16
altimeter + drifter mean + 0.1 ms^{-1}	0.28
altimeter (2°S- 2°N)	0.25

180° and 2°N, 125°W) have large biases between the CWDs and the drifter mean.

The biases between the CWDs and the current estimators may result from an error in the scatterometer or TAO wind speed, interannual variations in currents (not parameterized by the SOI), or vertical shear in the water column. Because winds in the TAO array are predominantly westward, the bias would correspond to QuikSCAT wind speeds being on average 0.1 ms^{-1} higher than the TAO winds, after accounting for currents, a relatively small error and well within the expected measurement errors of either. Alternatively, if the bias is from vertical shear, then the zonal surface currents are more eastward (generally, weaker) than the currents at 15 m.

The coefficients used for the altimeter estimator are given in Table 2 for each TAO buoy. The coefficients include the drifter mean plus 0.1 ms^{-1}. An estimator for the zonal surface currents, U_s, needed to correct zonal anemometer winds U in air-sea flux bulk formulas or for scatterometer-buoy comparisons, can be constructed for any time using (3) and these coefficients. To obtain relative zonal motion, $U - U_s$, the estimate of U_s must be subtracted from the absolute (zonal) wind U (e.g., anemometer wind). The meridional component would be unchanged because, as discussed below, no meridional current estimator has significant skill.

6. Meridional velocities

Meridional CWDs are noisier than their zonal counterparts. The analysis is difficult because the TIW signal is probably overwhelming any mean, seasonal or interannual signal in the meridional velocity. Also, Ekman drift transitions to downwind drift approaching the equator; this dynamical shift starts poleward of 2°N and 2°S. Finally, the geostrophic velocities may exceed actual velocities near the equator, as mentioned in the previous section.

The meridional geostrophic current anomalies, in fact, have no skill in estimating the meridional CWDs and the skill of the drifter estimates (which include an Ekman current component) is quite small. Although

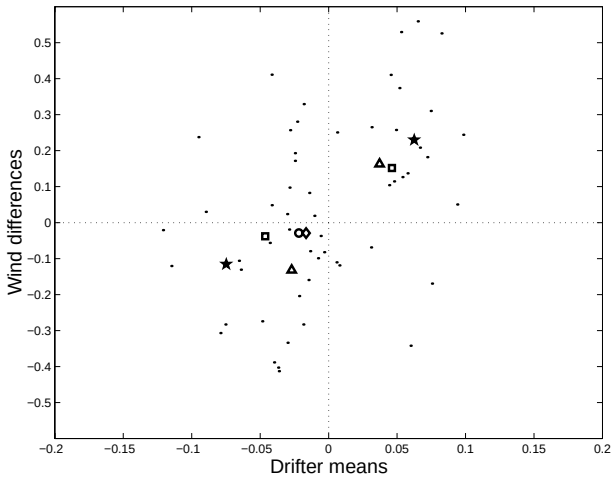

Figure 4. Meridional means of drifters and CWDs at each buoy. Latitude binned means show poleward velocities at 8°(triangles), 5°(squares), and 2°(stars). Equatorial means for the drifters (circle) and for the moored ADCP data (diamond).

not predictable, the meridional CWDs are just as energetic as the zonal CWDs. The overall rms values for the zonal and meridional CWDs are 0.41 and 0.43 ms^{-1}, respectively.

The means of the meridional CWDs for each buoy, plotted against the meridional drifter means (Figure 4), show considerable scatter. Bin-averaging the means by latitude reveals that meridional CWD means generally exceed drifter means by about a factor of two and that both estimates of mean currents are poleward, creating a mean divergence about the equator, as seen in Figure 1. The drifter velocities are at 15-m depth, and the wind difference velocity estimates are at the surface. Ekman dynamics suggest that the latter should be larger than the former. However, the magnitudes of the CWD vectors are significantly larger than would be expected from an oceanic Ekman response (Ralph and Niiler, 1999). We were unable to find a systematic relationship between the time series of CWDs and the wind stress that would establish that they are in fact an Ekman response.

7. Application to Scatterometer Validation

In situ wind observations are routinely used to validate the empirical model function used to convert radar backscatter to wind vectors. Buoy winds have been used extensively in these efforts and the TAO array contributes a large fraction of available buoy winds. With-

Table 2. Coefficients for zonal surface currents

lon	lat	c	a_1	ϕ_1	a_2	ϕ_2	b	lon	lat	c	a_1	ϕ_1	a_2	ϕ_2	b
137E	0	0	0	0	0	0	0.49	155W	8S	0.01	0.06	1.55	0	0	-0.05
137E	2N	0.09	0.41	1.37	0.20	-0.60	-0.42	155W	5S	-0.14	0	0	0	0	-0.11
137E	5N	0.48	0.16	-1.05	0	0	-0.04	155W	2S	-0.15	0.22	2.40	0.22	1.36	-0.14
137E	8N	-0.03	0.09	-1.11	0.07	2.74	0.06	155W	0	-0.04	0.23	-2.75	0.29	1.30	-0.24
147E	0	0.10	0.18	2.24	0.15	-0.33	-0.15	155W	2N	-0.24	0.51	-2.12	0.36	1.16	-0.26
147E	2N	0.12	0.23	2.17	0.18	-0.28	-0.23	155W	5N	0.18	0	0	0	0	-0.20
147E	5N	0.35	0.19	0.10	0	0	-0.07	155W	8N	0.31	0.34	0.98	0.11	-2.46	-0.01
156E	5S	0.01	0.11	1.25	0	0	-0.10	140W	8S	-0.05	0	0	0.05	-0.59	-0.07
156E	2S	-0.08	0.31	1.91	0.22	-0.23	-0.23	140W	5S	-0.16	0	0	0.08	1.73	-0.11
156E	0	0.13	0.23	2.31	0.23	0.09	-0.18	140W	2S	0.02	0.21	2.70	0.22	1.64	-0.08
156E	2N	0.05	0.25	2.52	0.23	0.17	-0.26	140W	0	0.01	0.25	-2.33	0.33	1.72	-0.23
156E	5N	0.30	0.17	0.48	0	0	-0.08	140W	2N	-0.30	0.56	-1.85	0.41	1.75	-0.26
156E	8N	0.09	0.19	-0.23	0.08	2.46	0.01	140W	5N	0.12	0	0	0.15	-0.16	-0.17
								140W	9N	0.19	0.27	1.00	0.06	3.06	-0.03
165E	8S	0.11	0.17	-0.76	0	0	0	125W	8S	-0.05	0.04	0.11	0	0	-0.07
165E	5S	0.02	0.15	1.54	0	0	-0.15	125W	5S	-0.21	0.08	0.23	0	0	-0.10
165E	2S	-0.09	0.35	2.19	0.27	0.17	-0.21	125W	2S	0.03	0.19	3.11	0.20	1.61	-0.10
165E	0	0.08	0.27	2.72	0.26	0.29	-0.22	125W	0	-0.02	0.29	-1.99	0.26	2.05	-0.24
165E	2N	0.05	0.32	3.06	0.24	0.19	-0.32	125W	2N	-0.50	0.61	-1.58	0.32	2.38	-0.26
165E	5N	0.26	0.15	1.05	0	0	-0.11	125W	5N	0.08	0.13	-1.45	0	0	-0.16
165E	8N	0.09	0.21	0.07	0.05	2.81	0.04	125W	8N	0.38	0.36	0.91	0.11	-0.31	-0.02
180	8S	0.06	0.12	0.13	0	0	-0.06	110W	8S	-0.08	0.08	0.02	0.05	-1.15	-0.06
180	5S	-0.05	0.13	1.87	0.07	0.09	-0.12	110W	5S	-0.22	0.07	0.60	0	0	-0.10
180	2S	-0.10	0.34	2.28	0.22	0.70	-0.19	110W	2S	0.07	0.18	-2.53	0.23	1.58	-0.15
180	0	-0.13	0.28	2.98	0.22	0.64	-0.26	110W	0	-0.06	0.38	-1.71	0.23	2.08	-0.26
180	2N	-0.19	0.42	-2.74	0.26	0.34	-0.33	110W	2N	-0.44	0.61	-1.34	0.21	2.47	-0.24
180	5N	0.25	0.13	0.90	0.10	-0.28	-0.15	110W	5N	0.23	0.19	-0.01	0.19	-0.20	-0.12
180	8N	0.18	0.27	0.51	0.09	2.74	0.04	110W	8N	0.12	0.31	1.53	0	0	-0.04
170W	8S	0.04	0.10	0.73	0	0	-0.06	95W	8S	-0.02	0.05	0.31	0.05	0.08	-0.03
170W	5S	-0.10	0.11	2.11	0.07	0.97	-0.10	95W	5S	-0.11	0	0	0.06	2.12	-0.08
170W	2S	-0.15	0.27	2.37	0.21	0.80	-0.13	95W	2S	0.01	0	0	0.17	1.92	-0.15
170W	0	-0.11	0.21	-3.06	0.26	0.78	-0.23	95W	0	-0.09	0.27	-1.22	0	0	-0.21
170W	2N	-0.25	0.40	-2.36	0.32	0.67	-0.28	95W	2N	-0.27	0.49	-1.04	0	0	-0.14
170W	5N	0.22	0	0	0	0	-0.16	95W	3.5	0.07	0.20	-0.78	0	0	-0.09
170W	8N	0.27	0.33	0.72	0.08	3.06	0	95W	5N	0.39	0	0	0.10	0.49	-0.07
								95W	8N	0.17	0.28	1.90	0.10	0.94	-0.01
								95W	10N	0.05	0.07	1.15	0	0	0.02
								95W	12N	0.03	0.16	-1.11	0.05	-2.94	0

out a current correction, TAO buoy wind comparisons suggest that the QuikSCAT winds are too weak in the 3–10 ms^{-1} range, by the amount of the mean differences shown in Figure 1a. This apparent bias could be even larger if a period of only a few months is used for the comparison; ocean currents can be as large as 1 ms^{-1} at many of the TAO buoy locations over a period of several months.

To illustrate the importance of removing the currents, we compared daily TAO winds with wind vectors from the SeaWinds scatterometer on the Japanese Midori (ADEOS-II) satellite. Calibration and preliminary validation of the SeaWinds instrument was based on only a few months of data (F. Wentz and D. Smith, personal communication, 2003) (Figure 5). These efforts require a timely comparison, which may preclude the availability of simultaneous current measurements. Therefore, the climatological estimators are particularly relevant for this application.

For three TAO buoys along 155°W (Figure 5), SeaWinds data within 25 km were screened for rain and data from the problematic outer swath edges were eliminated. Nearby screened data from a single swath (up to four vectors) were averaged and then the time series of vectors were filtered using a five-day running mean. The TAO anemometer winds were also filtered using the five-day running mean. Zonal scatterometer winds were subtracted from zonal TAO winds, and the CWDs were filtered using a two-month running mean. At each buoy we used the coefficients in Table 2 and (4) to compute an estimate of the zonal current. The SOI index[1] is customarily boxcar-averaged over a five-month period; for this example, we averaged the SOI index over the five-month period spanning the observations. For each buoy the smoothed CWDs are shown (solid) along with the climatological current estimate (dashed). In all cases the mean westward current and its seasonal variations reproduce qualitatively the smoothed CWDs.

8. Conclusions

We compared three-year mean and monthly zonal surface currents in the tropical Pacific Ocean with collocated differences between absolute winds measured from anemometers on TAO buoys and relative winds measured by the satellite-based QuikSCAT scatterometer. Mean zonal CWDs resemble the mean currents from 15-m deep drifters; however, mean meridional CWDs are much larger than mean meridional drifter currents. The divergence of the mean CWDs (Figure 1) about the equator is suggestive of an Ekman response.

[1]ftp://ftp.bom.gov.au/anon/home/ncc/www/sco/soi/soiplaintext.html, divided by 10

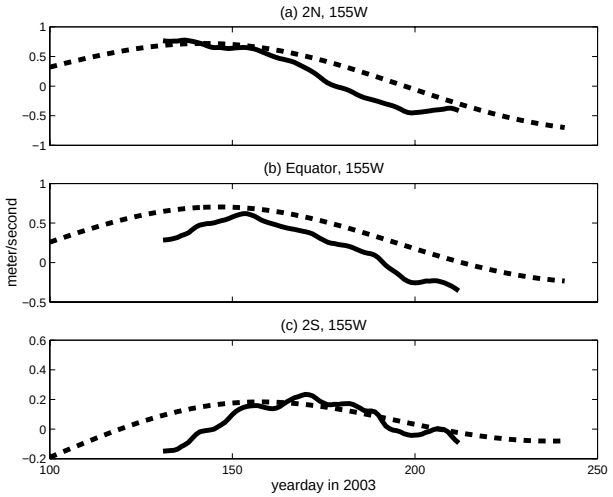

Figure 5. Example of estimator for SeaWinds on Midori. Zonal component of daily TAO buoy wind minus scatterometer wind (solid) from SeaWinds on Midori and altimeter estimator (dashed) along 155°Wat (a) 2°N, (b) the equator, and (c) 2°S.

Between 2°S and 2°N, where currents are relatively large, collocated wind differences (CWDs) agree qualitatively with near-surface currents from ADCP, current meters, and monthly surface geostrophic current anomalies from the TOPEX/Poseidon altimeter. At higher latitudes, the agreement is less clear.

The CWDs are also compared with climatological current estimators from drifters at 15-m depth, shipboard ADCP, and the geostrophic currents. Climatological estimators are used for drifter and ADCP data, owing to relatively sparse spatial and temporal sampling. The estimators consist (where available) of a mean, an annual and a semi-annual harmonic, and a factor related to the Southern Oscillation Index (SOI). The drifter and ADCP magnitudes are considerably smaller than those of the altimeter and the CWDs, apparently the result of spatial smoothing. There is a significant reduction in CWD variance (skill) by subtracting either the altimeter or drifter estimators. However, the ADCP estimator does not significantly reduce the variance. There is a mean bias between the drifters and the CWDs, with drifters approximately 0.1 ms^{-1} more westward. It cannot be determined from these data whether this bias is from the winds or from the currents.

Meridional wind data and estimators show poor agreement with the meridional CWDs, consistent with previous unsuccessful attempts by Johnson et al. (2002) to characterize the meridional currents. Large, but unpredictable, currents have been attributed primarily to

tropical instability waves. The meridional CWDs here have magnitudes nearly as large as the zonal component.

We provide (Table 2) the coefficients necessary to construct time-varying zonal current estimates at most TAO buoy locations: amplitudes and phases of the annual and semi-annual harmonics as well as the SOI regression coefficient from the altimeter data and the mean from the drifter data. When subtracted from an absolute (zonal) wind measurement, these time-varying surface current estimators give an estimate of relative motion, comparable to a scatterometer wind. The relative motion can be used to correctly implement bulk formulas (e.g., Liu et al., 1979) for computing air-sea fluxes, as well as to improve comparisons between scatterometer and buoy winds.

Acknowledgments. We thank the QuikSCAT project and PODAAC for scatterometer winds, the TAO Project Office for buoy winds and other meteorological variables, Dudley Chelton and Michael Schlax at OSU for the altimeter data, and Remote Sensing Systems for SSM/I data collocated with QuikSCAT. KAK and SD were supported by NASA's Ocean Vectors Winds Science Team (contract 1216233 with the Jet Propulsion Laboratory). GCJ was supported by the NOAA Office of Oceanic and Atmospheric Research and the NOAA Office of Global Programs. PMEL Contribution Number 2648.

References

Bonjean, F., G.S.E. Lagerloef, 2002. Diagnostic model and analysis of the surface currents in the tropical Pacific Ocean, *J. Phys. Ocean., 32,* 2938-2954.

Dickinson, S., K.A. Kelly, M.J. Caruso, and M.J. McPhaden, 2001. A note on s between the TAO buoy and NASA scatterometer wind vectors, *J. Atmos. and Ocean. Technol, 18,* 799-806.

Freitag, H.P., M. O'Haleck, G.C. Thomas, and M.J. McPhaden, 2001. Calibration procedures and instrumental accuracies for ATLAS wind measurements. *NOAA. Tech. Memo. OAR PMEL-119,* NOAA/Pacific Marine Environmental Laboratory, Seattle, Washington, 20 pp.

Huddleston, J.N., R.D. West, S.H. Yueh, and Y.T. Wu, 1996. Advanced techniques for improving wind direction ambiguity removal in scatterometry, *IGARSS, '96*, Remote Sensing for a Sustainable Future, (Cat. No. 96CH35875). IEEE, New York, NY, USA; 1718-1720.

Johnson, G. C., B. M. Sloyan, W. S. Kessler, and K. E. McTaggart. 2002. Direct measurements of upper ocean currents and water properties across the tropical Pacific Ocean during the 1990's. *Prog. in Ocean., 52,* 31-61.

Johnson, G. C. 2001. The Pacific Ocean subtropical cell surface limb. *Geophys. Res. Lett., 28,* 1771-1774.

Kelly, K.A., S. Dickinson, M.J. McPhaden, and G.C. Johnson, 2001. Ocean currents evident in satellite wind data, *Geophys. Res. Lett., 28*, 2469-2472.

Kelly, K. A., S. Dickinson, and Z.-J. Yu, 1999. NSCAT tropical wind stress maps: Implications for improving ocean modeling, *J. Geophys. Res. - Oceans*, **104**, 11,291–11,310.

Lagerloef, G.S.E., G.T. Mitchum, R.B. Lukas and P.P. Niiler, 1999. Tropical Pacific near-surface currents estimated from altimeter, wind and drifter data, *J. Geophys. Res., 104,* 23313-23326.

Liu, W.T., K.B. Katsaros, and J.A. Businger, 1979. Bulk parameterization of air-sea exchanges of heat and water vapor including the molecular constraints at the interface, *J. Atmos. Sci., 36,* 1722-1735.

Quilfen, Y., B. Chapron, and D. Vandemark, 2001. The ERS scatterometer wind measurement accuracy: Evidence of seasonal and regional biases, *J. Atmos. and Ocean. Tech., 18,* 1684-1697.

Ralph, E.A., and P.P. Niiler, 1999. Wind-driven currents in the Tropical Pacific, *J. Phys. Ocean., 29,* 2121-2129.

Yu, Lisan, R.A. Weller, and B. Sun, 2004. Improving latent and sensible heat flux estimates for the Atlantic Ocean (1988-99) by a synthesis approach, *Journal of Climate*, **17**, 373–393.

Wentz, F.J., and D.K. Smith, 1999. A model function for the ocean-normalized radar cross section at 14 GHz derived from NSCAT observations, *J. Geophys. Res.*, **104**, 11499-11514.

Kathryn A. Kelly, Applied Physics Laboratory, University of Washington, Box 355640, Seattle, WA 98195, USA. (kkelly@apl.washington.edu)

This preprint was prepared with AGU's LaTeX macros v5.01, with the extension package 'AGU++' by P. W. Daly, version 1.6b from 1999/08/19.